Sesquiterpene from Polygonum Barbatum Disrupt Mitochondrial Membrane Potential to Induce Apoptosis and Inhibits Metastasis by Downregulating Matrix Metalloproteinase and Osteopontin in NCI-H460 Cells

Binte Zehra
Dr Panjwani Center for Molecular Medicine and Drug Research
Ayaz Ahmed (ayaz.ahmed@iccs.edu)
Dr Panjwani Center for Molecular Medicine and Drug Research https://orcid.org/0000-0001-8792-7850
Ajmal Khan
University of Nizwa
Afshan Shams
Dr Panjwani Center for Molecular Medicine and Drug Research
Reaz Uddin
Dr Panjwani Center for Molecular Medicine and Drug Research
Sidra Rafi
Dr Panjwani Center for Molecular Medicine and Drug Research
Taseer Ahmed Khan
University of Karachi
Umar Farooq
COMSATS Institute of Information Technology - Abbottabad Campus
Syed Abid Ali
University of Karachi HEJ Research Institute of Chemistry

Research Article

Keywords: Sesquiterpene, metastasis, angiogenesis, osteopontin, caspases, MMP-2/9

Posted Date: December 29th, 2021

DOI: https://doi.org/10.21203/rs.3.rs-1187353/v1

Abstract

Background: Globally, lung cancer accounts for 18% of cancer-associated mortalities. Among the subtypes, non-small-cell lung cancer (NSCLC) is the most prevalent one. The increased resistance and poor survival rates, signifies disease aggressiveness and thus require a search for an alternative anticancer molecule.

Hypothesis/Purpose: Earlier, the isolated sesquiterpene i.e. compound **1** ((E)-Methyl 6-acetoxy-7-methoxy-1-(2-methylpropylidene)-1H-indene-3-carboxylate) from *P. barbatum* was isolated, characterized by us and reported for preliminary anticancer activity. Considering its potent activity, this study was designed to explore the underlying molecular mechanism of apoptosis and metastasis against NCI-H460 cells.

Method: The molecular mechanism of compound **1** inducing apoptosis and inhibiting metastasis was elucidated by analyzing mitochondrial membrane potential, DNA fragmentation, clonogenic assay, invasion assay and expression of apoptotic (Caspases 3, 6, 8, 9 and BAK) and metastatic markers (MMP 2, 9 and osteopontin).

Results: Compound **1** significantly inhibited cell proliferation and induced apoptosis *via* intrinsic route i.e. the mitochondrial pathway by disrupting mitochondrial membrane potential. The enhanced expression of caspases 6, 9, BAK and HRK with downregulation of Bcl-2L1 and Ki67 further confirmed the involvement of the intrinsic apoptotic pathway. Moreover, compound **1** restricted the invasive nature of NCI-H460 cells evinced by reduced cell invasion in Boyden chamber invasion assay and downregulating the expression of metastatic markers i.e. matrix metalloproteinase 2 / 9 and VEGF. It was also found that it blocks osteopontin by negatively regulating its expression; a marker protein in cancer management.

Conclusion: Conclusively, this sesquiterpene exhibited potent anticancer and anti-metastatic activity and can be explored further as possible pharmacophores

Introduction

Cancer is defined as a state where transformed cells grow beyond boundaries by surpassing major regulatory pathways. These rampantly growing cells form a mass i.e. tumor on the primary site and further infiltrate other organs, thereby causing damage to them. Cancer is a global concern with a high mortality rate and reduced life expectancies. According to recent estimates, 19.3 million new cancer cases were registered in 2020 with over 10.0 million deaths reported worldwide (Globocan 2021). Among different cancer types, lung cancer is the second most diagnosed cancer (11.4 million) after breast (11.7 million) and ranked number one among the cancer related mortalities i.e. 18% in 2020 (Globocan 2021). In Pakistan, lung cancer is the third most diagnosed cancer and stands second in cancer-related mortalities in 2020 (Globocan 2021). Among lung cancer types, non-small-cell lung cancer (NSCLC) constitutes 85% of overall lung cancers each year, with high recurrence rates even after undergoing curatively intended surgery at an early stage (Islami et al., 2015). Despite the advanced strides in NSCLC therapy, including neo-adjuvant and personalized treatments, critical challenges still prevail because of

tumor metastasis, drug resistance, and low survival rates (Herbst et al., 2008). Therefore, there is a persuasive need for new chemotherapeutic agents or unique therapeutic modalities to overcome the situation.

The uncontrolled growth of cells avoiding apoptosis and metastasis are the two hallmarks of cancer. Usually, cells undergo apoptosis as programmed cell death which involve coordinated expression of different proteins. Apoptosis usually occurs *via* intrinsic (mitochondrial) and extrinsic (death receptor) pathways. During the intrinsic pathway, mitochondrial outer membrane permeabilized in response to stimulus which results in the release of cytochrome c to form apoptosome. This further activates initiator (8, 9 or 10) and executioner (3, 6 and 7) caspases to initiate apoptosis. Proteins of the Bcl-2 family are well known markers that are involved in apoptosis and are categorized into pro-apoptotic (Bax, Bak) and anti-apoptotic (Bcl-2L1 or Bcl-XL) regulators. The regulator interacts with each other and determines whether the cell will survive or undergo apoptosis (Adams & Cory, 1998). BCl-2L1 prevents apoptosis by avoiding mitochondrial membrane permeabilization by inhibiting BAK or BAX activator. On the other hand, BAX induces mitochondrial membrane permeabilization and marks cells for apoptosis. HRK (harakiri) is another pro-apoptotic gene that promotes apoptosis *via* intrinsic pathways by inhibiting BCL-2L1 and other anti-apoptotic genes. The coordination of genes to promote apoptosis can be visualized as rounding, blebbing, shrinkage, nuclear-size reduction, and formation of apoptotic bodies under a microscope (Elmore, 2007). Thus, any molecule that promotes apoptosis can act as a desirable cancer-preventing strategy.

Malignant cells have a capacity to metastasize i.e. evade from their origin to other body healthy organs and destroy them through the lymphatic system (Alizadeh et al., 2014). Cell migration is useful for many physiological conditions especially wound healing, but in cancer, it affects vital organs like the brain, bones, lungs, etc. (Hulkower & Herber, 2011; Ma et al., 2016). Osteopontin (OPN), a recently gained interest protein in cancer research, an extracellular matrix multifaceted protein has recently gained interest in cancer research and has been found to be overexpressed in different carcinomas. It was also found to be associated with several receptors mediated signaling pathways and controls various characteristic features of cancer such as extracellular matrix remodeling, cancer invasion and metastasis to distant organs of the body (Zhao et al., 2018; Hao et al., 2019). It is also reported to modulate the cancer microenvironment by interacting with matrix metalloproteinase i.e. MMP-2 and 9 thus promoting metastasis. The level of osteopontin positively correlates with the grade of cancer state (Hao et al., 2019). Thus, osteopontin being a master regulator can also act as a therapeutic target for diagnosis and can be targeted to device novel anticancer therapies.

Many anticancer drugs available in the market including, vincristine, vinblastine, and paclitaxel are either the natural product or their synthetic analogues. Natural flora-derived products and their derivatives have provided anticancer drugs for decades with fully elucidated molecular mechanisms (Harvey et al., 2015). Since, the natural compounds hold key importance in the discovery of anticancer or anti-metastatic compounds, by virtue of their biodiversity, they can be a hope for the development of new cancer drugs. Reports indicate that secondary metabolites such as flavonoids, flavones, and sesquiterpenes isolated

from different plant sources showed better pharmacological properties than the synthetic chemical structures (Kinghorn et al., 2016). Similarly, extracts and isolated pure compounds from *Polygonum barbatum* showed cholinergic, antinociceptive, anti-tumor, anti-inflammatory, anti-venom, and diuretic activities. Recently, our group reported the isolation, characterization, and anticancer potential of the isolated novel sesquiterpene ((E)-Methyl 6-acetoxy-7-methoxy-1-(2-methylpropylidene)-1H-indene-3-carboxylate) from *P. barbatum* referred to as compound **1** which was found active against NSCLC (NCI-H460) cells (Farooq et al., 2017). Compound **1** was found to be selectively cytotoxic against the cancer cells as evident by apoptotic and migration assay (Farooq et al., 2017). However, its complete molecular mechanism by which it exhibits apoptotic and anti-metastatic activity are yet to be explored. Therefore, the aim of current study was to evaluate the in-depth apoptotic and metastatic inhibiting potential of compound **1** and to underpin its molecular mechanism in NCI- H460 cells.

Methodology

Sample collection and identification

The whole plant of *Polygonum barbatum* (5.4 kg) was collected from Northern areas (Mansehra), Khyber Pakhtunkhwa Pakistan in October 2015. The plant was identified by Dr. Manzoor Ahmed (Taxonomist), at the Department of Botany, Government Postgraduate College, Abbottabad, Pakistan. A voucher specimen (No. 66130) has been submitted in herbarium of the same department.

Extraction and Isolation

The aerial part of the plant material was shade dried, ground into fine powder and extracted thrice with methanol (3 x 10L) at room temperature and filtered. The filtrate was subjected to vacuum rotary evaporator to get crude extract (245 g). The whole extract was further partitioned into three fractions, namely *n*-hexane (85 g), ethyl acetate (48 g) and *n*-butanol (94 g).

The ethyl acetate fraction was chromatographed on silica gel (E. Merck, 230– 400 mesh and 70 –230 mesh) using the solvents with increasing polarity, *n*-hexane was used with gradient of ethyl acetate up to 100% followed by methanol, which resulted in sub-fractions depending on the polarity of compounds. Sub-fractions number 4—10 out of the total 12, were further, subjected to column chromatography to get compound **1** (7.5 mg) at EtOAc: *n*-hexane (27:73) (Figure S1).

Cell Culture:

The non-small cell lung carcinoma cells NCI-H460 (ATCC, USA) were used in the study. The cell line was routinely passaged, sub-cultured, and maintained in RPMI culture media as ideally describes by us (Farooq et al., 2017).

Mitochondrial Membrane Potential Assay:

To demonstrate the disruption of mitochondrial membrane potential, 1 x 10^6 cells per well were seeded in a 6 well plate and incubated overnight at 37^{o}C in 5% CO_2 environment. The next day, the drug was added and the plate was further incubated for 48h. After the incubation period, nutritionally exhausted media was aspirated off and cells monolayer was detached by trypsinization. Cells pellet were washed, re-suspended, and stained with 1µL JC-1 (tetraethylbenzimidazolylcarbocyanine iodide; Thermo, USA) dye at 37^{o}C for 30 min. Later, the dye was removed, and stained cells were collected through centrifugation at 400 x g for 5 min which was then analyzed for change in mitochondrial potential using flow cytometer FACSCalibur (Beckton Dickinson). The dye JC-1 was excited at 520nm, whereas fluorescence was measured at 590 nm. During cell sorting, 10,000 events per sample were recorded as one experimental reading and the percentage of cells in each quadrant was analyzed using CellquestPro Software. Unstained and stained untreated cells were used as controls to adjust the voltages of the red/green filters, while carbonyl cyanide m-chlorophenyl hydrazone (CCCP) was used as a positive inducer of MMP disruption in H460 cells.

DNA Fragmentation Assay:

To observe the post-treatment nuclear changes, 1 x 10^5 cells were seeded in 6 well plate containing coverslip and incubated overnight. The next day, cells were treated with different concentrations of the compound and further incubated for 48h in 5% CO_2 humidified incubator. Post incubation, coverslips were washed with phosphate buffer saline (PBS) and the cells were fixed for 15 min with 2 mL 3.7% formaldehyde followed by 4',6-diamidino-2-phenylindole (DAPI) staining (1:1000) for 10 min. The coverslips were analyzed and imaged at 400x total magnification by using a Nikon 90i fluorescence microscope (Nikon, Japan).

Invasion Assay:

Transwell inserts (8 µm pore size; Millipore, USA) were coated with geltrex (9 mg/mL; Thermo Scientific, USA) to form a membrane matrix. NCI-H460 cells (40,000) were seeded in the incomplete media with and without compound **1** at IC_{50} and IC_{70} concentrations for 30 min at 37^{o}C. Then the transwell was placed in 24 well plate containing 500 µL complete culture media as a chemoattractant. Finally, the plate was incubated for 48h at 37 ^{o}C in 5% CO_2 environment. Post incubation, the matrix was carefully removed, and invaded cells were fixed with 3.7% formaldehyde for 15 min. After fixation, the invaded cells were stained with crystal violet and then observed and photographed at 4x magnification under an inverted microscope (Nikon TE2000, Japan).

Zymography:

The change in the enzymatic activity of MMP 2 and 9 after the treatment with compound **1** was analyzed through gelatin zymography; performed following the same procedure as described previously (Zehra et al., 2019).

Expression Analysis:

The gene and protein expression profile of the caspases family (3, 6, 8, and 9) apoptotic markers (Bcl-2L1, BAK, HRK), metastatic markers (MMP 2 and 9), and master regulator osteopontin were analyzed through RT-PCR and immunocytochemistry. For RT-PCR, cellular mRNA from treated and control cells was isolated and converted to cDNA which was later amplified for respective genes and quantified using Image J as described earlier (Zehra et al., 2019). The cells treated with compound **1** were fixed and analyzed for protein expression by evaluating mean fluorescence intensity after immunocytochemical staining as described previously (Zehra et al., 2019), and then observed under fluorescent microscope at 100× total magnification.

Clonogenic Assay:

Evaluation of recurrence potential of NCI-H460 cells post-treatment with compound **1** was demonstrated through clonogenic assay. For this purpose, 8,000 cells were plated and allowed to grow at 37^{o}C in a CO_2 incubator in a 6 well plate. After 24h, cells were treated with compound **1** at IC_{50} and IC_{70} concentration for 48h in 5% CO_2 atmosphere. Later, the drug was removed; cells were washed, transferred in the complete culture media conditions and incubated for further 20 days to allow cells growth. While on every 3rd day, fresh culture media was periodically added to the wells post PBS washing. After the incubation, cells were fixed with 3.7% formaldehyde and crystal violet staining was performed.

Chorioallantoic Membrane Assay:

Fertilized eggs were utilized for the development of *ex ovo* angiogenic model to assess the neovascularization potential of the test compound. Incubation of the eggs was performed at 37^{o}C with a narrow apex pointing down and 180^{o} rotation after every 6h. At embryo development day 4 (EDD4), eggs were wiped with 75% ethanol and an estimated 3 mm hole was made in the eggshell at the narrow apex. Adhesive tape was used to cover the hole to avoid contamination and desiccation. The incubation of the fertilized eggs was carried out under the same growth conditions and stationary phase, with a narrow apex facing upward. At EDD8, the egg holes were further enlarged to 1 - 2 cm and filter paper containing 30 µL test compound was placed around the vascular junction. The eggshell window was sealed with adhesive tape and eggs were incubated at 37^{o}C until EDD11. Post incubation, the vascular junction was photographed and observed for neovascularization.

Computational studies

Compound Preparation

The 2D structure coordinates of compound **1** were sketched and retrieved as mol format and consequently converted into 3D coordinates by using the Balloon program (Vainio & Johnson, 2007). Energy minimization was performed using FROG2 (Miteva et al., 2010) to remove clashes among atoms

of the ligand and to develop a reasonable starting pose and attain the near-global minimum of the compound's conformation.

Protein Modeling and Quality assessment

The 3D structure of osteopontin (OPN) is not available and has not been solved yet. Therefore, in the absence of the 2D structure, ab-initio structure prediction approach was used to predict the tertiary structure of Osteopontin using I-Tasser (Iterative Threading ASSEmbly Refinement) (Yang et al., 2015). The UniProt database was used to retrieve the OPN fasta format sequence having identifier number P10451 (“UniProt: A Hub for Protein Information,” 2015). The C-score is a confidence score for estimating the quality of the predicted model by I-Tasser. It is typically in the range of −5, and 2, where a higher score reflects a better quality of the model. The structure was also subjected to reFold refinement server. The server attempts to identify and fix likely errors in provided 3D models of proteins via successive rounds of refinement. The quality assessment of predicted protein structure was performed by PROCHECK (Laskowski et al., 1993). The DoGSiteScorer was used for the binding site prediction of predicted model protein (Volkamer et al., 2012).

Molecular Docking

The molecular docking was performed using Auto Dock Vina version 1.5.6 supported by the MGL tool (Trott & Olson, 2010). It is designed to predict how small molecules, such as substrates or drug candidates, bind to a target structure. The predicted tertiary structure of OPN was docked with compound **1** (sesquiterpene). The structure was centered in a grid box having 24.30 Å, 15.72 Å, and 8.13 Å, by setting the number of points in each dimension X, Y, and Z, respectively and 0.758 Å spacing between the points. The Lamarckian genetic algorithm was implemented (Morris et al., 2009), and the parameters were set to the number of conformations 200 while the population size was 250 with a maximum number of energy evaluations set to 2500000 and number of generations to 27000. The rate of gene mutation was 0.02.

Statistical Analysis:

Data presented in this study is mean ± S.D. of triplicate experiments. While the statistical significance of the comparison between the treated and control groups was done using one-way ANOVA and p-value < 0.05 was referred to as significant.

Results

Compound **1** was isolated as light brown gummy solid with molecular formula $C_{18}H_{20}O_5$ suggested by NMR and ESI-MS, from ethyl acetate fraction of *Polygonum barbatum*. The characterization was done by using various spectroscopic techniques as well as through literature comparison and their detail spectroscopic data was published in our pervious article (Farooq et al., 2017).

Compound 1 Induce Apoptosis via intrinsic pathways i.e. disrupting Mitochondrial Membrane Potential:

Previously, compound **1** was found to have targeted apoptotic potential against NCI-H460 lung cancer cells but its mechanism i.e., either inducing intrinsic or extrinsic pathway was unknown. It was observed that after treatment with the compound, a significant cell population underwent the apoptotic or necrotic phase (Farooq et al., 2017). Complementary to these findings, the results from the current study showed significantly increased disruption of mitochondrial membrane potential after treatment with compound **1**. At IC_{50} (20 µM) and IC_{70} (40 µM) almost 58% to 70% population of cells respectively indicating an impaired mitochondrial potential as compared to the untreated control. However, the loss of MMP in the treated cells was comparable with the positive internal control i.e., CCCP, a protonophore that impaired mitochondrial potential in at least 75% of the cell population after 48h of treatment (Figure 1A and B). These results suggest compound **1** might trigger an intrinsic pathway to induce apoptosis in cancerous cells.

Fragmented nuclei with apoptotic bodies with the reduced nuclear area are the distinctive features of apoptotic cells in comparison to viable cells. DNA fragmentation was also noticed in the cells treated with compound **1** at IC_{50} and IC_{70} concentrations (Figure 2A and B). After 24h of treatment, the nuclear factor area of treated cells was significantly reduced by four times as compared to normal cells. However, after 48h the nuclear material significantly collapses as observed under the fluorescence microscope. Treated cells after 24h, reducing nuclear area factor of 0h cells to 4 times in the given time. However, complete nuclear collapse forming DNA debris was observed under the microscope after 48h treatment. Fragmented nuclei with apoptotic bodies were also evident in treated cells.

The cancerous cells have a characteristic feature to reproduce to form colonies after treatment with drugs; referred to as clonogenicity. The NCI-H460 cells were reported for potential clonogenicity, however, it was affected after treatment with the compound at IC_{50} and IC_{70} concentrations. The treated cells when further incubated in complete cell culture media for 20 days, the recurrence of cancer cells was not observed at any point. On the other hand, cells in control wells yielded a large number of the cell population as colonies (Figure 3A). The reduced protein expression of proliferation marker i.e. Ki67 was significantly downregulated after treatment with IC_{50} and IC_{70} concentrations of compound **1**, this further highlighted the anti-proliferative potential of this pharmacophore (Figure 3B).

The gene and protein expression analysis further concluded that treatment with compound **1** triggered an intrinsic pathway of apoptosis. After treatment, the gene expression analysis was also conducted for intrinsic (i.e. Caspases 3, 6, and 9) and extrinsic pathways (i.e. Caspase 8) markers. The result showed significantly increased expression of caspases 3, 6, and 9, whereas, down regulated expression of caspase 8 (Figure 4A and B). Compound **1**, significantly upregulated the gene expression of pro-apoptotic (BAK, HRK), on the contrary it downregulated the BCL-2L1 expression which is an anti-apoptotic gene (Figure 4A and B). The immunocytochemical analysis further confirmed activation of intrinsic pathway i.e., the protein expression of BCL2-L1, caspases 3 and 6 were increased, but expression of caspase 8 was reduced (figure 5A and B) in treated NCI-H460 cells (Figure 5A, B and Figure S2).

Compound 1 displays anti-metastatic potential:

Metastasis is an another hallmark of cancer that often results in the spread of cancer to a distant organ of the body and is responsible for tumor relapse (Steeg, 2016). Therefore, the isolated sesquiterpene (compound **1**) was also evaluated for anti-migratory or invasive effects against NCI-H460 cells. In our initial report, this compound was found to inhibit cell migration evident by reduced closure of scratch after treatment as compared to control (Farooq et al., 2017). In continuation to this, an invasion assay was performed to further consolidate the anti-metastatic potential of this compound using a transwell invasion assay coated with an artificial basement membrane. After treatment with compound at IC_{50} and IC_{70} concentrations, cells were significantly confined to the upper portion of the membrane and only a few cells breach the matrix through the well. However, untreated cells showed metastatic potential by significantly breaching the artificial basement membrane (Figure 6A).

On the other hand, both phenotypic (zymography)and genotypic (mRNA) levels of MMP 2 and 9 were also significantly down regulated in the treated NCI-H460 cells (Figure 6B, C, and D).

Anti-angiogenic activity of compound 1 against NCI-H460 cells:

Considering the anti-metastatic potential of compound **1**, its anti angiogenic potential was also evaluated. The results displayed that after implanting compound **1** containing filter paper on the neo-vascular junction, the process of formation of new blood vessels was substantially inhibited and the chick egg at EDD 11 had disrupted the blood circulatory system (Figure 7). Vascular endothelial growth factor (VEGF) is an angiogenic marker which was significantly downregulated after treatment with compound **1** at IC_{50} and IC_{70} concentration (Figure 6A and B).

Compound 1 Downregulate Osteopontin a Key regulator for Apoptosis and Metastasis:

In various cancers, osteopontin emerged as a multifactorial protein responsible to activate downstream pathways to promote proliferation, invasion, and migration. Our results showed the upregulation of osteopontin gene and protein expression in untreated NCI-H460 cells (Figure 8A - C). However, after treatment with compound **1**, its expression was downregulated by 70 – 80% at 20 and 40 µM doses, respectively. Thus, the molecular result was further confirmed using computational studies. The tertiary structure of osteopontin was built using an an-initio approach using I-Tasser, as its structure was not available in the database (Figure 9). The I-Tasser provided the top five protein models with different C-scores, numbers of decoys, and cluster density (Table -1) The 3D structure of osteopontin obtained was found to have significant similarity with the structure of OPN reported previously (Sivakumar & Niranjali Devaraj, 2014). The Dog Site Scorer was used for this purpose which predicted the top five binding pockets in which pocket P_0 is the most potential one and showed a 0.79 drug score and 0.63 simple scores (Figure S3; Table S1). Interestingly, the docking results also confirmed that isolated sesquiterpene (compound **1**) might lead to the suppression of osteopontin by binding with the nitrogen atoms of Lys 70 and Gln 71 with the oxygen atoms of compound 1 having a distance of 1.7 Å and 2.1 Å as shown in Figure 10A-C.

Discussion

Sesquiterpenes are the subclass of terpenes that are widely known for their diverse bioactivities against various microorganisms, cancer cell lines, tumor xenograft models, inflammatory and/or immunomodulatory models, etc. (Dahham et al., 2015; Flewelling et al., 2015; Formisano et al., 2017). However, very few reports have been published to date showing its potential apoptotic and anti-metastatic activities against NCI-H460 cells. Previously, our group for the first time reported the isolation and characterization of novel sesquiterpenes from the aerial parts of *P. barbatum* followed by preliminary anticancer and anti-metastatic activity against lung carcinoma cells (NCI-H460) (Farooq et al., 2017). The findings demonstrated that compound **1**, ((E)-Methyl 6-acetoxy-7-methoxy-1-(2-methylpropylidene)-1H-indene-3-carboxylate), selectively target cancer cells (IC_{50} = 17.86 ± 0.76 μM) compared to normal cells (IC_{50} = 30.32 ± 0.93 μM) evaluated using MTT assay and phase-contrast microscopy. Based on the previous understandings, the current study is focused on the demonstration of in-depth apoptotic and anti-metastatic activities of this compound followed by unveiling its underlying molecular mechanism.

Mitochondria are referred to as an energy house of the cells, however, it also initiate signals to induce cell apoptosis. It releases cytochrome c, a key regulator of apoptosome formation which in turn activates caspases and proteases to initiate apoptosis (Gottlieb et al., 2003). JC-1 staining is utilized to evaluate the disruption in mitochondrial membrane potential of the cells treated. It is a lipophilic, cationic, and green fluorescent dye which enters into healthy mitochondria to form J aggregate which excites in red spectra. However, in unhealthy or apoptotic cells mitochondria have a less negative charge due to increased membrane permeability, which also allows dye internalization but to a lesser extent. This reduced concentration of dye fails to form J aggregate and retains its original green fluorescence (Kaisar et al., 2018). JC-1 staining of cells treated with compound **1** at IC_{50} and IC_{70} concentrations showed the significant collapse of mitochondrial membrane potential (MMP, $\Delta\psi m$), as evident by enhanced green fluorescence, thus, indicating caspase-dependent apoptosis in NCI-H460 cells (Figure 1A and B). Alongside, the mitochondrial membrane potential, nuclear changes i.e., DNA fragmentation occurs which is also an ultimate step of apoptosis and takes the cells to the death phase (Elmore, 2007). Compound **1** significantly alters the nuclear integrity as evident by collapsed and nuclear debris under a fluorescence microscope after treatment at higher concentrations i.e. 40 μM (Figure 2A and B). Caspases play an important role either in intrinsic or extrinsic pathways of apoptosis after inducing membrane potential. Compound **1** was significantly found to upregulate the expression of caspases 6 and 9 involved in the intrinsic pathway (Figure 3 and 4). On the contrary, it was found to downregulate the expression of caspase 8, a marker of extrinsic pathway (Figure 3 and 4). Although various reports demonstrated the simultaneous activation of both apoptotic death receptor (extrinsic) and mitochondrial pathways (intrinsic) by different sesquiterpenes in several cancer cells, including NSCLC cells to bring out massive apoptosis in tumor cells (Babaei et al., 2018; Kabeer et al., 2013). On the contrary, compound **1** promotes the intrinsic pathway more as compared to the extrinsic pathway as evidenced by RT-PCR and immunocytochemical results. Compound **1** was also found to increase pro apoptotic (BAK) gene expression with the decrease in anti-apoptotic Bcl-2L1 expression (Figure 4 and 5). Based on the

observations, it was assumed that compound **1** upon triggering the cellular damage, activated the mitochondrial pathway of apoptosis which in response stimulated mitochondrial membrane potential disruption followed by enhanced BAK activation and BCL2-L1 inhibition. Upon BAK/BAX dimerization, caspases 9 undergo proteolytic cleavage, hence apoptosis is induced, and nuclear machinery is degraded by nucleases leading to cell membrane disruption and formation of apoptotic bodies (Kiraz et al., 2016). Furthermore, compound **1** treated cells when grown in complete growth media for 20 days, showed no recurrence of cancer cells reducing its clonogenic ability after 48h treatment as compared to control cells (Figure 3A). It also downregulated the cell proliferation marker i.e., Ki-67 which further evinced the reduced proliferation or clonogenicity of NCI-H460 cells after treatment (Figure 3B). Our results are in connection with the results of Cidado et al (2016), indicating that Ki-67 is directly correlated with clonogenic or metastatic properties of the cancer cells. Ki-67 depleted cells had a proliferative disadvantage in colony formation assay as compared to the wild-type cells (Cidado et al., 2016).

Tumor metastasis is a key step in the process of tumorigenesis, being responsible for enhanced morbidity and mortality. When cancer starts to grow and develops into a mass, it leaves its original site and enters the circulation to metastasize to other parts of the body (Popper, 2016). Mostly lung cancer cells establish metastases in bone, liver, and brain. Variety of changes at the molecular level promotes metastasis which includes epithelial-mesenchymal transition i.e., destruction of adhesive nature of cell-matrix, breakdown of basement protein by matrix metalloproteinase (MMP) and new vascularization by vascular endothelial growth factors (VEGF) (Quintero-Fabian et al., 2019). Therefore, the majority of the effort in current research focuses on the inhibition of the biomarkers that promotes metastasis to effectively combat the recurrence and resistance of cancers (van Zijl et al., 2011). Thus, this study also addresses the role of the isolated sesquiterpene i.e. compound **1**, as a potent anti-metastatic agent. In previous results, this compound inhibits migration in the scratch assay (Farooq et al., 2017). However, the inhibition of the invasive nature of NCI-H460 cells is yet to be elucidated which accounts for rupturing basement matrix and moved to distance organs. Compound **1** was found to inhibit invasive properties of NCI- H460 cells in a Boyden chamber invasion assay. It is the most convenient in vitro method to evaluate the metastatic properties (invasiveness) of the cells as it employs an artificial basement matrix and nutrients enriched media as a chemoattractant (Massague & Obenauf, 2016). When the cells were treated with IC_{50} and IC_{70} concentration of compound **1**, it significantly inhibited the invasive nature of cells as evident by only a few cells invading the matrix membrane and were found on the other side of the chamber as compared to control cells with marked enhanced invasive properties (Figure 6A). Since, the matrix metalloproteinase is the key marker to aid invasion during metastasis, the expression levels of the enzymes were also evaluated post 48h treatment (Massague & Obenauf, 2016). The results revealed that compound **1** inhibited the enzyme activity and gene expression of both MMP2 and 9, as analyzed by gelatin zymography and RT-PCR (Figure 6B – D). Tumor cells require a continuous supply of nutrients and oxygen to develop into a cancer mass which is usually supplied by blood vessels (Bielenberg & Zetter, 2015). Considering the anti-metastatic nature of compound **1** with downregulation of VEGF expression, its anti angiogenic activity was determined using the chorioallantoic membrane (CAM) model. This model has been used to study the anti-angiogenic effects of various test compounds as it

offers the possibility to conveniently estimate their preclinical response in naturally immune-deficient chick eggs (Lokman et al., 2012). The compound was found to be anti-angiogenic as evident by a significant reduction in the process of neovascularization as well as inhibition in the advancement of already existing blood vessels to new ones (Figure 7).

Osteopontin, a phosphorylated glycoprotein, was found to play a crucial role in cancer development and progression. Its level was found to be increased in various cancer types and it serves as a biomarker for the detection of any cancer within the body (Johnson et al., 2003; Lamort et al., 2019). Recently, osteopontin has received much attention because of its central functionality in regulatory and physiological pathways thus inhibiting apoptosis and promoting metastasis, angiogenesis, and bone remodeling pathways (Lorand & Graham, 2003; Mangala et al., 2007; Nishimichi et al., 2011; O'Regan & Berman, 2000). Osteopontin via CD44/integrin receptors, directly upregulates mutant p53 and downregulates cellular destruction proteins i.e., BAK and BAX, thereby shutting down the natural process of programmed death of dysfunctional cells (Klement et al., 2018). While on the contrary, it promotes the metastatic cascade by positively regulating MMP and VEGF (Lin et al., 2015). Since the apoptotic and anti-metastatic nature of compound **1** was demonstrated earlier in the study, its effect on osteopontin expression was also evaluated. The results of immunocytochemical and gene expression analysis indicated that the master regulator of apoptosis and metastasis, OPN was significantly down regulated in the treated cells in comparison to the control HCI-H460 cells (Figure 8). Furthermore, osteopontin is being highlighted for its crucial importance as a biomarker and involvement in cancer development and metastasis, therefore, its predicted 3D model was also constructed using computational tools. The predicted model of osteopontin shows the highest C-scores. The literature proposed the hypothetical structure of OPN, and it was found quite similar to the predicted model 2 and shown high similarity with bone sialoprotein (Johnson et al., 2003). The structure was refined with refolding to remove the atomic clashes between the atoms and fix the side chains and loop structure of a protein (Figure S4) while the quality of the predicted model was demonstrated using Ramachandran plot (Figure S5). The predicted binding pocket P_0 contains a total of 42 residues. However, the more frequently found residues are Asp, Ser, Gln, Asn, and Glu. The observed molecular interaction by docking depicts strong hydrogen bonding between the protein and the ligand. As a result, the protein was cleaved at Pro137 to produce N and C terminal fragments, as shown in Figure 10A. Several earlier studies have reported the importance of Lys and Gln in full-length osteopontin protein (Lorand & Graham, 2003; Nishimichi et al., 2011). The reports highlighted that Gln and Lys enhance the biological activity of OPN and aid cross-linking of the enzyme transglutaminase during OPN polymerization. These two residues play an essential role in developing the metastatic phenotype during breast cancer by increasing cytokine expression (Mangala et al., 2007; Nishimichi et al., 2011). Hence, the fragmentation and binding of compound 1 can affect the osteopontin mechanism by deregulation and suppressing its activity towards metastasis progression. The binding energy of compound **1** indicates the strong binding affinity between the protein and compound **1**, as illustrated in Figures 10A and B. Compound **1** has the lowest binding energy of -5.25 kcal/mol, (refer to Table S2). The binding pockets of both the clusters are the same (i.e., P_0) in the protein tertiary structure. Hence, it further ensures the drugable binding pockets as potential drug binding sites. The enhanced OPN

expression is associated with multiple cancers and the favorable binding interactions of compound 1 as depicted by docking scores is indicating that it is a logical approach for cancer control.

Conclusion

In conclusion, several reports highlighted the role of sesquiterpenes lactones as an anticancer lead but to the best of our knowledge, very few non-lactone sesquiterpenes are referred as potent anticancer hits to date (Chao et al., 2019). However, the novel sesquiterpene, compound 1 bearing indene ring, and its lipophilic nature showed potential anticancer activity in addition to its roles as apoptosis-inducing and anti-metastatic agents. Thus, with the support of existing literature, a schematic pathway was illustrated (Figure 11). Compound **1** can be explored further in vivo or preclinical studies as a potential anticancer agent

Abbreviations

CCCP; Carbonyl cyanide m-chlorophenyl hydrazone, CAM; Chorioallantoic membrane, DAPI; 4',6-diamidino-2-phenylindole, EDD4; embryo development day 4, MMP; Matrix Metalloproteinases, NSCLC; Non-small-cell lung cancer, OPN; Osteopontin, PBS; Phosphate buffer saline, VEGF; Vascular endothelial growth factors,

Declarations

Ethics approval

Not applicable

Consent to Participate

Not applicable

Consent for publication

Not applicable.

Author Statement

BZ, AA, AS, RU, SR, and TAK: Conceptualization, Methodology, Perform Experiment, collect data and first draft preparation. **AK,** UF: Provided compound **1, *AA and SAA***: Supervision, manuscript editing and finalization. **All authors read and approved the manuscript and all data were generated in-house and that no paper mill was used.**

Funding:

The authors are grateful to International Center for Chemical and Biological Sciences for providing partial financial support for this work.

Competing interests

The authors declare that they have no competing interests.

Availability of Data and Material

Data will be available on request

References

1. Adams, J. M., & Cory, S. 1998. The Bcl-2 protein family: arbiters of cell survival. Science (New York, N.Y.), 281(5381), 1322–1326. https://doi.org/10.1126/science.281.5381.1322
2. Alizadeh, A. M., Shiri, S., & Farsinejad, S. 2014. Metastasis review: from bench to bedside. Tumor Biology, 35(9), 8483–8523. https://doi.org/10.1007/s13277-014-2421-z
3. Babaei, G., Aliarab, A., Abroon, S., Rasmi, Y., & Aziz, S. G. 2018. Application of sesquiterpene lactone: A new promising way for cancer therapy based on anticancer activity. Biomed Pharmacother, 106, 239–246. https://doi.org/S0753-3322(18)30988-0
4. Bielenberg, D. R., & Zetter, B. R. 2015. The Contribution of Angiogenesis to the Process of Metastasis. Cancer J, 21(4), 267–273. https://doi.org/10.1097/PPO.0000000000000138
5. Chao, W. W., Cheng, Y. W., Chen, Y. R., Lee, S. H., Chiou, C. Y., & Shyur, L. F. 2019. Phyto-sesquiterpene lactone deoxyelephantopin and cisplatin synergistically suppress lung metastasis of B16 melanoma in mice with reduced nephrotoxicity. Phytomedicine, 56, 194–206. https://doi.org/S0944-7113(18)30562-2
6. Cidado, J., Wong, H. Y., Rosen, D. M., Cimino-Mathews, A., Garay, J. P., Fessler, A. G., Rasheed, Z. A., Hicks, J., Cochran, R. L., Croessmann, S., Zabransky, D. J., Mohseni, M., Beaver, J. A., Chu, D., Cravero, K., Christenson, E. S., Medford, A., Mattox, A., de Marzo, A. M., … Park, B. H. 2016. Ki-67 is required for maintenance of cancer stem cells but not cell proliferation. Oncotarget, 7(5), 6281–6293. https://doi.org/10.18632/oncotarget.7057
7. Dahham, S. S., Tabana, Y. M., Iqbal, M. A., Ahamed, M. B., Ezzat, M. O., Majid, A. S., & Majid, A. M. 2015. The Anticancer, Antioxidant and Antimicrobial Properties of the Sesquiterpene beta-Caryophyllene from the Essential Oil of *Aquilaria crassna*. Molecules, 20(7), 11808–11829. https://doi.org/10.3390/molecules200711808
8. Elmore, S. 2007. Apoptosis: a review of programmed cell death. Toxicol Pathol, 35(4), 495–516. https://doi.org/10.1080/01926230701320337
9. Farooq, U., Naz, S., Zehra, B., Khan, A., Ali, S. A., Ahmed, A., Sarwar, R., Bukhari, S. M., Rauf, A., Ahmad, I., & Mabkhot, Y. N. 2017. Isolation and characterization of three new anti-proliferative Sesquiterpenes

from *Polygonum barbatum* and their mechanism *via* apoptotic pathway. BMC Cancer, 17(1), 694. https://doi.org/10.1186/s12885-017-3667-9

10. Flewelling, A. J., Bishop, A. I., Johnson, J. A., & Gray, C. A. 2015. Polyketides from an Endophytic *Aspergillus fumigatus* Isolate Inhibit the Growth of *Mycobacterium tuberculosis* and *MRSA*. Nat Prod Commun, 10(10), 1661–1662.
11. Formisano, C., Samna, C., Ballero, M., Chianese, G., Sirignano, C., Rigano, D., Millan, E., Munoz, E., & Taglialatela-Scafati, O. 2017. Anti-inflammatory sesquiterpene lactones from *Onopordum illyricum* L. (Asteraceae), an Italian medicinal plant. Fitoterapia, 116, 61–65. https://doi.org/10.1016/j.fitote.2016.11.006
12. Gottlieb, E., Armour, S. M., Harris, M. H., & Thompson, C. B. 2003. Mitochondrial membrane potential regulates matrix configuration and cytochrome c release during apoptosis. Cell Death Differ, 10(6), 709–717. https://doi.org/10.1038/sj.cdd.4401231
13. Hao, C., Cui, Y., Chang, S., Huang, J., Birkin, E., Hu, M., Zhi, X., Li, W., Zhang, L., Cheng, S., & Jiang, W. G. 2019. OPN promotes the aggressiveness of non-small-cell lung cancer cells through the activation of the RON tyrosine kinase. Scientific Reports, 9(1), 18101. https://doi.org/10.1038/s41598-019-54843-2
14. Harvey, A. L., Edrada-Ebel, R., & Quinn, R. J. 2015. The re-emergence of natural products for drug discovery in the genomics era. Nat Rev Drug Discov, 14(2), 111–129. https://doi.org/10.1038/nrd4510
15. Herbst, R. S., Heymach, J. v, & Lippman, S. M. 2008. Lung cancer. N Engl J Med, 359(13), 1367–1380. https://doi.org/10.1056/NEJMra0802714
16. Hulkower, K. I., & Herber, R. L. 2011. Cell Migration and Invasion Assays as Tools for Drug Discovery. Pharmaceutics, 3(1), 107–124. https://doi.org/10.3390/pharmaceutics3010107
17. Islami, F., Torre, L. A., & Jemal, A. 2015. Global trends of lung cancer mortality and smoking prevalence. Transl Lung Cancer Res, 4(4), 327–338. https://doi.org/10.3978/j.issn.2218-6751.2015.08.04
18. Johnson, G. A., Burghardt, R. C., Bazer, F. W., & Spencer, T. E. 2003. Osteopontin: roles in implantation and placentation. Biol Reprod, 69(5), 1458–1471. https://doi.org/10.1095/biolreprod.103.020651
19. Kabeer, F. A., Sreedevi, G. B., Nair, M. S., Rajalekshmi, D. S., Gopalakrishnan, L. P., Kunjuraman, S., & Prathapan, R. 2013. Antineoplastic effects of deoxyelephantopin, a sesquiterpene lactone from *Elephantopus scaber*, on lung adenocarcinoma (A549) cells. J Integr Med, 11(4), 269–277. https://doi.org/jintegrmed2013040
20. Kaisar, M. A., Sivandzade, F., Bhalerao, A., & Cucullo, L. 2018. Conventional and electronic cigarettes dysregulate the expression of iron transporters and detoxifying enzymes at the brain vascular endothelium: *In vivo* evidence of a gender-specific cellular response to chronic cigarette smoke exposure. Neurosci Lett, 682, 1–9. https://doi.org/10.1016/j.neulet.2018.05.045
21. Kinghorn, A. D., Blanco, D. E. E. J., Lucas, D. M., Rakotondraibe, H. L., Orjala, J., Soejarto, D. D., Oberlies, N. H., Pearce, C. J., Wani, M. C., Stockwell, B. R., Burdette, J. E., Swanson, S. M., Fuchs, J. R.,

Phelps, M. A., Xu, L., Zhang, X., & Shen, Y. Y. 2016. Discovery of Anticancer Agents of Diverse Natural Origin. Anticancer Res, 36(11), 5623–5637. https://doi.org/10.21873/anticanres.11146

22. Kiraz, Y., Adan, A., Kartal Yandim, M., & Baran, Y. 2016. Major apoptotic mechanisms and genes involved in apoptosis. Tumour Biol, 37(7), 8471–8486. https://doi.org/10.1007/s13277-016-5035-9
23. Klement, J. D., Paschall, A. v, Redd, P. S., Ibrahim, M. L., Lu, C., Yang, D., Celis, E., Abrams, S. I., Ozato, K., & Liu, K. 2018. An osteopontin/CD44 immune checkpoint controls CD8+ T cell activation and tumor immune evasion. J Clin Invest, 128(12), 5549–5560. https://doi.org/10.1172/JCI123360
24. Lamort, A. S., Giopanou, I., Psallidas, I., & Stathopoulos, G. T. 2019. Osteopontin as a Link between Inflammation and Cancer: The Thorax in the Spotlight. Cells, 8(8). https://doi.org/cells8080815
25. Laskowski, R. A., Moss, D. S., & Thornton, J. M. 1993. Main-chain bond lengths and bond angles in protein structures. J Mol Biol, 231(4), 1049–1067. https://doi.org/ 10.1006/jmbi.1993.1351
26. Lin, Q., Guo, L., Lin, G., Chen, Z., Chen, T., Lin, J., Zhang, B., & Gu, X. 2015. Clinical and prognostic significance of OPN and VEGF expression in patients with non-small-cell lung cancer. Cancer Epidemiol, 39(4), 539–544. https://doi.org/10.1016/j.canep.2015.05.010
27. Lokman, N. A., Elder, A. S., Ricciardelli, C., & Oehler, M. K. 2012. Chick chorioallantoic membrane (CAM) assay as an in vivo model to study the effect of newly identified molecules on ovarian cancer invasion and metastasis. Int J Mol Sci, 13(8), 9959–9970. https://doi.org/10.3390/ijms13089959
28. Lorand, L., & Graham, R. M. 2003. Transglutaminases: crosslinking enzymes with pleiotropic functions. Nat Rev Mol Cell Biol, 4(2), 140–156. https://doi.org/10.1038/nrm1014
29. Ma, Y., Pan, J.-Z., Zhao, S.-P., Lou, Q., Zhu, Y., & Fang, Q. 2016. Microdroplet chain array for cell migration assays. Lab on a Chip, 16(24), 4658–4665. https://doi.org/10.1039/C6LC00823B
30. Mangala, L. S., Fok, J. Y., Zorrilla-Calancha, I. R., Verma, A., & Mehta, K. 2007. Tissue transglutaminase expression promotes cell attachment, invasion and survival in breast cancer cells. Oncogene, 26(17), 2459–2470. https://doi.org/10.1038/sj.onc.1210035
31. Massague, J., & Obenauf, A. C. 2016. Metastatic colonization by circulating tumour cells. Nature, 529(7586), 298–306. https://doi.org/10.1038/nature17038
32. Miteva, M. A., Guyon, F., & Tuffery, P. 2010. Frog2: Efficient 3D conformation ensemble generator for small compounds. Nucleic Acids Res, 38(Web Server issue), W622-7. https://doi.org/gkq325
33. Morris, G. M., Huey, R., Lindstrom, W., Sanner, M. F., Belew, R. K., Goodsell, D. S., & Olson, A. J. 2009. AutoDock4 and AutoDockTools4: Automated docking with selective receptor flexibility. J Comput Chem, 30(16), 2785–2791. https://doi.org/10.1002/jcc.21256
34. Nishimichi, N., Hayashita-Kinoh, H., Chen, C., Matsuda, H., Sheppard, D., & Yokosaki, Y. 2011. Osteopontin undergoes polymerization in vivo and gains chemotactic activity for neutrophils mediated by integrin alpha9beta1. J Biol Chem, 286(13), 11170–11178. https://doi.org/10.1074/jbc.M110.189258
35. O'Regan, A., & Berman, J. S. 2000. Osteopontin: a key cytokine in cell-mediated and granulomatous inflammation. Int J Exp Pathol, 81(6), 373–390. https://doi.org/10.1046/j.1365-2613.2000.00163.x

36. Popper, H. H. 2016. Progression and metastasis of lung cancer. Cancer Metastasis Rev, 35(1), 75–91. https://doi.org/10.1007/s10555-016-9618-0 [pii]
37. Quintero-Fabian, S., Arreola, R., Becerril-Villanueva, E., Torres-Romero, J. C., Arana-Argaez, V., Lara-Riegos, J., Ramirez-Camacho, M. A., & Alvarez-Sanchez, M. E. 2019. Role of Matrix Metalloproteinases in Angiogenesis and Cancer. Front Oncol, 9, 1370. https://doi.org/10.3389/fonc.2019.01370
38. Sivakumar, S., & Niranjali Devaraj, S. 2014. Tertiary structure prediction and identification of druggable pocket in the cancer biomarker - Osteopontin-c. J Diabetes Metab Disord, 13(1), 13. https://doi.org/10.1186/2251-6581-13-13
39. Steeg, P. S. 2016. Targeting metastasis. Nat Rev Cancer, 16(4), 201–218. https://doi.org/10.1038/nrc.2016.25
40. Trott, O., & Olson, A. J. 2010. AutoDock Vina: improving the speed and accuracy of docking with a new scoring function, efficient optimization, and multithreading. J Comput Chem, 31(2), 455–461. https://doi.org/10.1002/jcc.21334
41. UniProt: a hub for protein information. 2015. Nucleic Acids Res, 43(Database issue), D204-12. https://doi.org/10.1093/nar/gku989
42. Vainio, M. J., & Johnson, M. S. 2007. Generating conformer ensembles using a multiobjective genetic algorithm. J Chem Inf Model, 47(6), 2462–2474. https://doi.org/10.1021/ci6005646
43. van Zijl, F., Krupitza, G., & Mikulits, W. 2011. Initial steps of metastasis: cell invasion and endothelial transmigration. Mutat Res, 728(1–2), 23–34. https://doi.org/10.1016/j.mrrev.2011.05.002
44. Volkamer, A., Kuhn, D., Rippmann, F., & Rarey, M. 2012. DoGSiteScorer: a web server for automatic binding site prediction, analysis and druggability assessment. Bioinformatics, 28(15), 2074–2075. https://doi.org/10.1093/bioinformatics/bts310
45. Yang, J., Yan, R., Roy, A., Xu, D., Poisson, J., & Zhang, Y. 2015. The I-TASSER Suite: protein structure and function prediction. Nat Methods, 12(1), 7–8. https://doi.org/10.1038/nmeth.3213
46. Zehra, B., Ahmed, A., Sarwar, R., Khan, A., Farooq, U., Abid Ali, S., & Al-Harrasi, A. 2019. Apoptotic and antimetastatic activities of betulin isolated from *Quercus incana* against non-small cell lung cancer cells. Cancer Manag Res, 11, 1667–1683. https://doi.org/10.2147/CMAR.S186956 cmar-11-1667

Tables

Table 1: The statistics of the I-Tasser provided top five protein models

Model	*C* - Score	Exp. TM-Score	Exp. RMSD	No. of Decoys	Cluster Density
1	-3.35	0.34 + -0.12	14.5+-3.7	1357	0.0339
2	-2.82			1267	0.0575
3	-3.08			703	0.0445
4	-3.76			639	0.0224
5	-5.00			229	0.0031

Figures

Figure 1

Mitochondrial membrane potential (MMP) of NCI H460 cells after treatment with compound **1**. (A) Flowcytometric analysis of mitochondrial membrane potential disruption, CCCP used as positive control (B) Graphical representation of membrane potential disruption by compound **1** after 48 hours of treatment (C) Compound **1** Structure. Statistical significance of the date was represented as ***$p < 0.001$ and *###*$p < 0.001$ as compared to vehicle control and CCCP, respectively.

Figure 2

Effect of compound **1** on the nuclear morphology (A) Nuclear fragmentation in NCI-H460 cells post 24h and 48h treatment, observed at 400x total magnification under a fluorescent microscope (B) Graphical representation of mean nuclear area factor. ***p < 0.001 and ###p < 0.001 represents data significance with untreated control and 24h results.

Figure 3

Recurrence of NCI-H60 cells after treatment with Compound **1**. (A) Demonstration of colony formation potential of Compound **1** untreated and treated NCI-H460 cells for 48h, which were later allowed to in culture media for 3 weeks. (B) Immunocytochemical staining for proliferative marker Ki-67 post 48h treatment with Compound **1**.

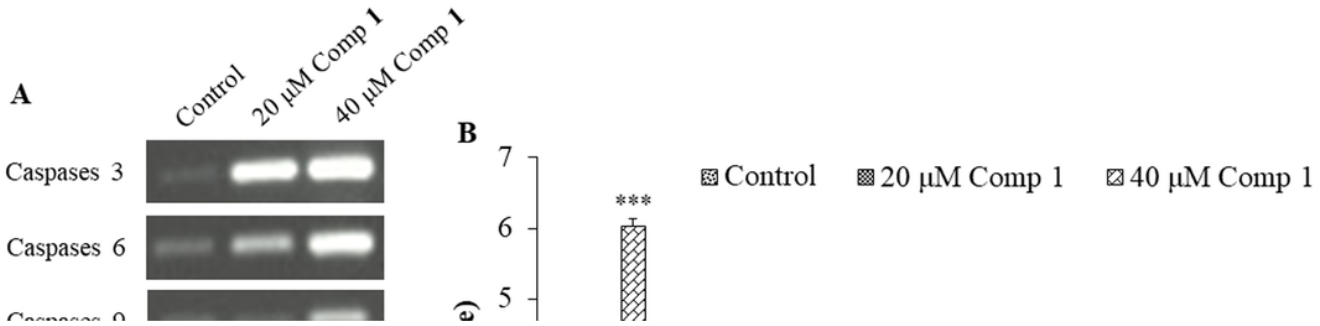

Figure 4

(A) Gene expression analysis of caspases family after treatment with compound **1**, GAPDH was used as a constitutive gene. (B) Quantitative analysis of differential gene expression of caspases 3, 6, 9, 8, BAK, BCL-2L1, and HRK. ***p < 0.001 versus untreated control.

Figure 5

Protein expression of marker proteins that are actively involved in tumorigenesis (A) Immunocytochemical staining for BCL-2L1, Caspases 3, 6, and 8 post 48h treatment with compound **1** (B) Quantitative representation of mean fluorescence intensity of the targeted proteins before and after the respective treatment. ***p < 0.001 indicates significance in contrast to untreated control.

Figure 6

Effect of compound **1** on metastatic potential of NCI-H460 cells (A) Effect of cell invasion after 48h treatment with compound **1**, invaded cells were visualized using crystal violet staining under 4x objective (B) Enzymatic activity of MMP2 and 9 (C) Gene expression of MMP2 and 9 (D) Graphical representation of the differential gene expression. Statistical significance of the data was represented as ***p < 0.001 as compared to control.

Figure 7

Evaluation of the anti-angiogenic potential of compound **1** through Chick Chorioallantoic Membrane (CAM) assay established as an ex ovo model.

Figure 8

Expression of osteopontin in NCI-H460 cells after treatment with compound **1** (A) Gene expression (B) Quantitative analysis of differential gene and protein expression of osteopontin (C) Immunocytochemical staining for osteopontin. Statistical significance of the data was presented as ***$p < 0.001$ versus untreated control.

Figure 9

Structure depiction of sesquiterpene and osteopontin target (A) Compound **1** (Sesquiterpene) structure by using Chemdraw (B) Osteopontin structure depicted by model 2 generated by I-Tasser server with the highest C- score.

Figure 10

The predicted structure of Osteopontin after docking with compound **1** performed by autodock Vina. (A): The docked structure depicts the effect of compound **1** on the OPN protein. It cleaved the protein into two fragments i.e. N and C terminal. (B) Shows the interactions between the OPN and compound **1**. It mediates two hydrogen bonds with Lys70 and Gln71 having distances of 1.7Å and 2.1Å, respectively (C) Histogram shows the binding energies of all conformations.

Figure 11

Proposed scheme of direct or indirect interaction of osteopontin with the targeted markers of the study considering existing literature.

Supplementary Files

This is a list of supplementary files associated with this preprint. Click to download.

- Figure1graph.xlsx
- Figure2graph.xlsx
- Figure4graphs.xlsx
- Figure5graphs.xlsx
- Figure6graph.xlsx
- Figure8graphs.xlsx
- SupplementaryMeterial.pdf